© 2015. Published by The Company of Biologists Ltd | Development (2015) 142, 2623-2632 doi:10.1242/dev.125336

RESEARCH ARTICLE

STEM CELLS AND REGENERATION

Perilipin$^+$ embryonic preadipocytes actively proliferate along growing vasculatures for adipose expansion

Ki Yong Hong[1], Hosung Bae[1], Intae Park[1], Dae-Young Park[1], Kyun Hoo Kim[1], Yoshiaki Kubota[2], Eui-Sic Cho[3], Hail Kim[1], Ralf H. Adams[4], Ook-Joon Yoo[1,*] and Gou Young Koh[1,*]

ABSTRACT

Despite the growing interest in adipose tissue as a therapeutic target of metabolic diseases, the identity of adipocyte precursor cells (preadipocytes) and the formation of adipose tissue during embryonic development are still poorly understood. Here, we clarified the identity and dynamic processes of preadipocytes in mouse white adipose tissue during embryogenesis through direct examination, lineage tracing and culture systems. Surprisingly, we found that lipid-lacking but perilipin$^+$ or adiponectin$^+$ proliferating preadipocytes started to emerge at embryonic day 16.5, and these cells underwent active proliferation until birth. Moreover, these preadipocytes resided as clusters and were distributed along growing adipose vasculatures. Importantly, the embryonic preadipocytes exhibited considerable coexpression of stem cell markers, such as CD24, CD29 and PDGFRα, and a small portion of preadipocytes were derived from PDGFRβ$^+$ mural cells, in contrast to the adult preadipocytes present in the stromal vascular fraction. Further analyses with *in vitro* and *ex vivo* culture systems revealed a stepwise but dynamic regulation of preadipocyte formation and differentiation during prenatal adipogenesis. To conclude, we unraveled the identity and characteristics of embryonic preadipocytes, which are crucial for the formation and expansion of adipose tissue during embryogenesis.

KEY WORDS: Adipogenesis, Adipose tissue, Angiogenesis, Preadipocytes

INTRODUCTION

The worldwide epidemic of obesity over the past half century has raised a surge of interest in the understanding of the origin, development, integrity and remodeling of adipose tissues (Rosen and MacDougald, 2006; Gesta et al., 2007; Cao, 2010; Wang et al., 2013). Two types of adipose tissues, which are different in structure and function, are found in mammals as white adipose tissue (WAT) and brown adipose tissue (BAT). WAT regulates energy storage and mobilization in the form of triacylglycerides, and has paracrine and endocrine functions via secretion of adipokines and growth factors, whereas BAT is specialized as an energy dissipater for heat during cold- and diet-induced thermogenesis. Recent reports (Wu et al., 2012; Rosenwald et al., 2013; Nedergaard and Cannon, 2014) reveal that WAT and BAT are interchangeable in certain pathophysiological situations, named 'browning' (WAT to BAT) and 'whitening' (BAT to WAT), indicating that adipose tissues are dynamic, versatile and communicative tissues. Nevertheless, the origin and development of adipose tissues are poorly understood.

Expansion of WAT during postnatal growth or obesogenic change in adults is primarily caused by appropriate or excessive filling of lipid into post-mitotic adipocytes, together with, although to a lesser extent, an ongoing proliferation and differentiation of preadipocytes, which are predominantly localized adjacent to adipose vasculatures (Nishimura et al., 2007; Li et al., 2011; Tran et al., 2012). By contrast, formation of WAT during embryonic development is assumed by serial processes of commitment of putative adipoblasts, mainly from mesoderm, and proliferation and differentiation of adipoblasts into adipocyte precursor cells (preadipocytes) (Gesta et al., 2007; Tang et al., 2008). These processes have been supposed to appear along the growing adipose vasculature, which is termed the 'adipose niche' (Crandall et al., 1997; Cho et al., 2007; Birsoy et al., 2011; Han et al., 2011). Although there have been attempts to characterize the distinct cellular intermediates (adipoblasts and preadipocytes) between mesodermal cells and differentiated adipocytes, such studies have been hampered by the lack of specific cell surface markers to identify and prospectively isolate them *in vivo*. A recent genetic approach using a lineage-tracing mouse model, the 'AdipoChaser mouse', demonstrated that most adipocytes could be committed and differentiated from their putative progenitors before birth (Wang et al., 2013). However, lineage tracing does not reveal details about phase timing and developmental cues. Moreover, changes in phenotypes in the long-term bring into question the ability to reliably identify phenotypic fingerprints based on observations at a single time point. Therefore, considering that substantial changes in phenotypes could be generated at an early time point by genetic changes and manipulations, it is valuable to observe embryonic tissues directly.

In this study, through direct examination of the embryonic inguinal fat pad, we explored the dynamic processes of identification and development of preadipocytes in inguinal WAT during embryogenesis. Unexpectedly, we found that the preadipocytes exist as perilipin$^+$ and adiponectin$^+$ cells either as lipid-lacking cells or small-sized lipid-containing cells, which are distributed as clusters along growing adipose vasculatures and are also highly proliferative, particularly at the periphery of the adipose cluster.

RESULTS

Emergence of perilipin$^+$ preadipocytes during embryogenesis

To explore the origin of preadipocytes *in vivo*, we attempted to identify the formation of WAT during murine embryonic development in the inguinal region, which is easily accessible

[1]Graduate School of Medical Science and Engineering, Korea Advanced Institute of Science and Technology (KAIST), Daejeon 305-701, Korea. [2]The Laboratory of Vascular Biology, Keio University, Tokyo 160-8582, Japan. [3]Laboratory for Craniofacial Biology, Cluster for Craniofacial Development and Regeneration Research, Chonbuk National University School of Dentistry, Jeonju 561-756, Korea. [4]Department of Tissue Morphogenesis, Max-Planck-Institute for Molecular Biomedicine, Faculty of Medicine, University of Münster, 48149 Münster, Germany.

*Authors for correspondence (gykoh@kaist.ac.kr; ojyoo@kaist.ac.kr)

Received 11 April 2015; Accepted 17 June 2015

Development (2015) 142, 2623-2632 doi:10.1242/dev.125336

compared with other regions, as well as being easily distinguishable by a developing lymph node at the center of a tripod-shaped vascular branch (Fig. 1A). As no specific markers for adipoblasts/preadipocytes are available, and there also is a possibility that a mixed population of adipoblasts/preadipocytes and perilipin 1^{+} matured adipocytes could exist in the developing adipose tissue, we traced prenatal adipogenesis by immunostaining of perilipin 1 (Plin1, hereafter called perilipin) in whole-mounted inguinal WAT (Fig. 1B; supplementary material Fig. S1A). At embryonic day (E) 14.5, neither apparent adipose tissue nor perilipin^{+} cells were observed (Fig. 1B). However, from E16.5, *de novo* lipid-lacking perilipin^{+} cells that were attached mainly along the CD31^{+} (Pecam1 – Mouse Genome Informatics) blood vessels started to appear (Fig. 1B). Remarkably, after two days, two different types of perilipin+ cells, either lipid-lacking or scant lipid droplet-containing cells that were stained with boron-dipyrromethene (BODIPY), were concomitantly increased and congregated into the shape of a cluster along the blood vessels (Fig. 1B,C). Moreover, the size of these clusters expanded profoundly without significant increases in cell sizes but with marked increase in the number of perilipin^{+} cells, which still had either no or small-sized lipid droplets, until postnatal day (P) 0 (Fig. 1C-F). These findings indicate that hyperplasia of perilipin^{+} cells was in progress in these clusters during the prenatal period. By contrast, lipid and other nutrients provided by nursing after birth (Rudolph et al., 2007) caused every perilipin^{+} cell to expand and change into lipid-filled perilipin^{+} adipocytes (Fig. 1C,D). Importantly, most of the growing CD31^{+} vascular network in the clusters highly expressed a key vascular growth factor receptor, VEGFR2 (Kdr – Mouse Genome Informatics), at E18.5 (Fig. 1G). Because perilipin has been known to be presented exclusively by lipid-filling adipocytes as a major isoform of lipid-coating proteins (Greenberg et al., 1991), our findings are unexpected because the putative preadipocytes also expressed perilipin either without any lipid droplets or with small lipid droplets. Based on these findings, we defined lipid-lacking or small lipid droplet-containing perilipin^{+} cells as 'perilipin^{+} preadipocytes' (PPAs), and fully differentiated, lipid-filled perilipin^{+} cells as 'perilipin^{+} matured adipocytes'.

Crucial interactions between PPA and their supporting vascular network during adipogenesis

Because PPA were relatively abundant along the distinct vascular networks but rarely existed in avascular regions in the adipose clusters at E16.5 (supplementary material Fig. S2A), we speculated that vasculatures provide an external cue for fate determination and differentiation of putative adipoblasts into PPA. To test our hypothesis, we generated endothelial *Vegfr2*-depleted mice

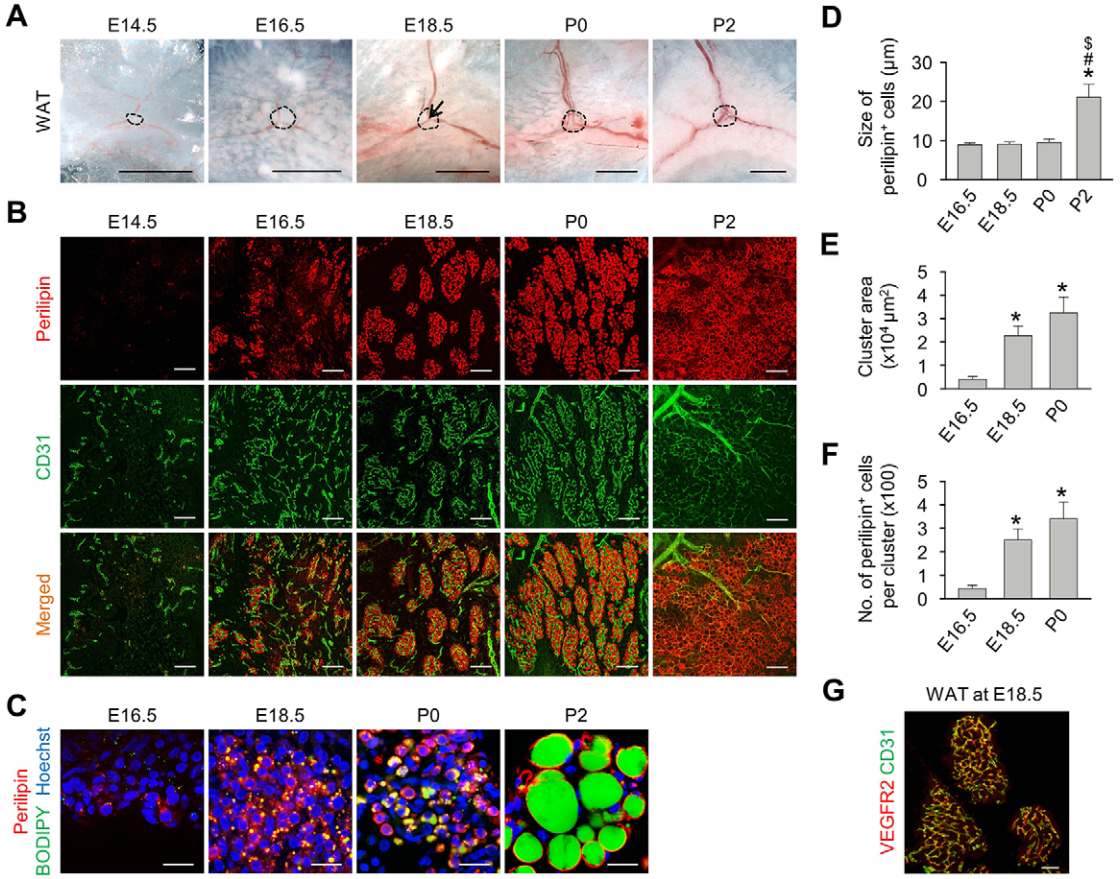

Fig. 1. Emergence of perilipin^{+} preadipocytes during embryogenesis. (A) Images showing inguinal WAT located around the developing inguinal lymph node (dashed circle) at the indicated time points. Arrow indicates tripod-shaped vascular branch. Scale bars: 500 μm. (B) Perilipin^{+} cells started to appear as clusters by E16.5, which grew and merged to become a whole adipose tissue composed of lipid-filling adipocytes at P2. Distinct vascular networks supporting the clusters are visualized by CD31 staining. Scale bars: 100 μm. (C) Images showing BODIPY^{+} lipid droplets coated with perilipin in the cytoplasm at the indicated time points. Scale bars: 25 μm. (D-F) Comparisons of the size of perilipin^{+} cells, cluster areas, and the number of perilipin^{+} cells per cluster at the indicated time points. *n*=5 per group. **P*<0.05 versus E16.5; $^{\#}$*P*<0.05 versus E18.5; $^{\$}$*P*<0.05 versus P0. Error bars represent s.d. (G) Image showing immunostaining of CD31^{+} and VEGFR2^{+} blood vessels in the adipose cluster at E18.5. Scale bar: 100 μm.

Development (2015) 142, 2623-2632 doi:10.1242/dev.125336

(VR2$^{\Delta EC}$) by intercrossing endothelial cell-specific *VE-cadherin-Cre*-ER^{T2} and *VEGFR2*$^{+/fl}$ mice, which enabled vascular disruption upon tamoxifen administration from E16.5. At E18.5, tamoxifen-treated VR2$^{\Delta EC}$ embryos showed hemorrhages and edema, indicating that these mice underwent effective vascular disruption owing to the loss of VEGFR2 in growing blood vessels, including inguinal adipose vasculature (Fig. 2A-C). In the inguinal region of these mice, the development of clusters was no longer prominent, and the number of PPAs per cluster had reduced by 49% compared with control embryos (Fig. 2C,D). Accordingly, the gene expression of *Vegfr2* and *Pparg2* (*Pparg* – Mouse Genome Informatics) in the WAT of VR2$^{\Delta EC}$ decreased by 77% and 62%, respectively (Fig. 2E,F). These findings demonstrate that endothelial-specific *Vegfr2* depletion was effective enough to induce vascular disruption, leading to the interruption of *in vivo* generation of PPA during adipogenesis.

Conversely, we generated *Col1a1-Cre/inducible COMP-Ang1*-Tg (Ang1^{OE}) mice that have connective tissue-driven overexpression of angiopoietin 1 (Ang1; Angpt1 – Mouse Genome Informatics) for a gain-of-function study on the developing adipose vasculatures. The gross appearance of E18.5 embryos of Ang1^{OE} was reddish compared with that of control embryos, suggesting increased blood vessel density and vessel enlargement (Fig. 2G). In the inguinal region, Ang1^{OE} embryos exhibited concomitantly expanded vascular network and clusters, and had a 2.1-fold increase in the number of PPAs per cluster (Fig. 2H-J). Moreover, the WAT of these embryos had 3.4-fold and 2.1-fold increases in the gene expression of *Vegfr2* and *Pparg2* compared with control embryos, respectively (Fig. 2K,L), indicating that adipose vasculature has a crucial relationship with *in vivo* adipogenesis during embryogenesis. Together, the embryonic distinct adipose vasculatures provide an external cue for the development of PPA and adipose tissue formation in a spatiotemporal manner.

Temporal but distinct changes of proliferative ability in PPA

To investigate whether active proliferation of PPA is an essential process for adipose growth during the prenatal period, we first stained the inguinal adipose tissues with a proliferation marker, PH3. In fact, a fair number of PH3^{+} cells that were noticeably matched with PPAs were observed from E16.5 to P0 (Fig. 3A; supplementary material Fig. S2B). Moreover, orthotopic-dissection image analysis revealed that most PH3^{+} PPAs were located at the periphery of the cluster at E18.5 (Fig. 3B). Second, using an alternative proliferation detection method, *in vivo* 5-ethynyl-2′-deoxyuridine (EdU) labeling, we confirmed that PPAs were actively proliferating at E18.5 (Fig. 3C; supplementary material Fig. S2C). Intriguingly, quantification revealed that the proportion of PH3^{+} cells in the PPA population in the cluster increased as the embryo got closer to birth (Fig. 3A,D). Furthermore, these findings were

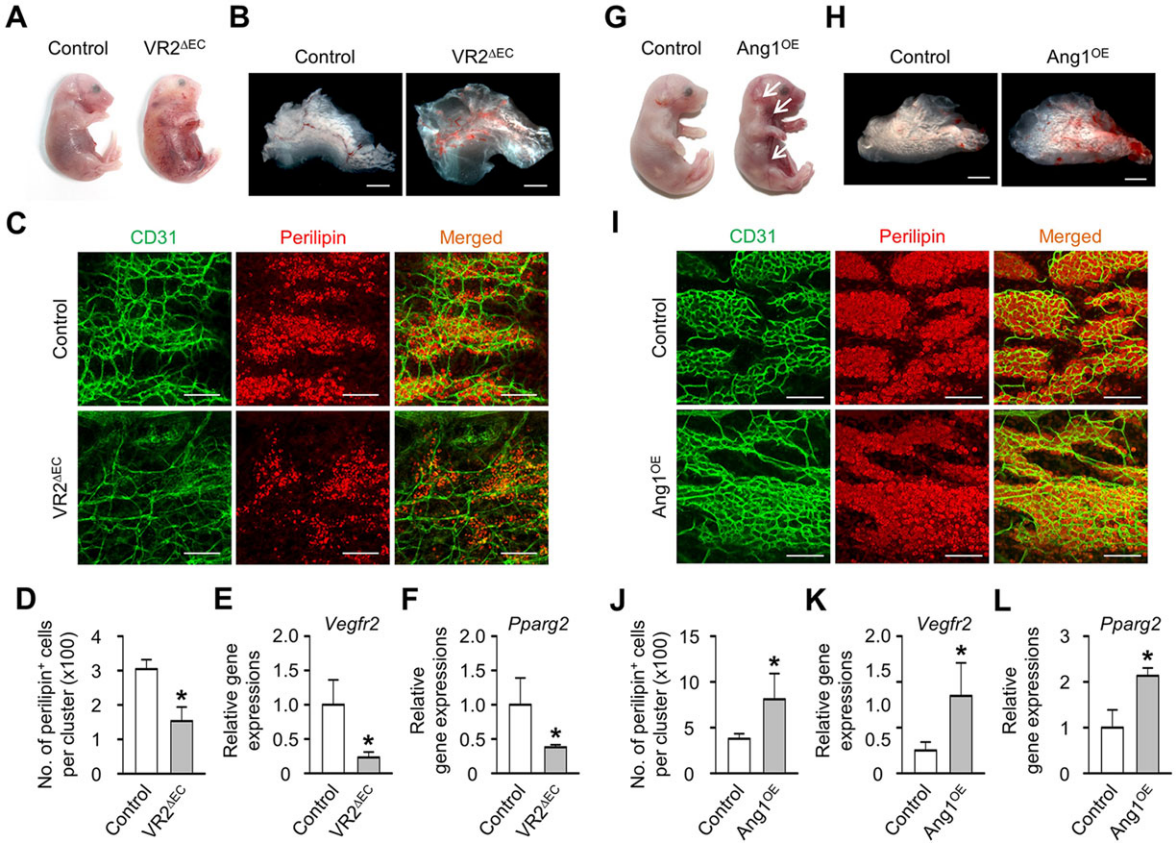

Fig. 2. Crucial interactions between PPAs and their supporting vascular network in adipogenesis. (A-L) The supporting vascular network was disrupted in VR2$^{\Delta EC}$ mice (A-F), whereas vascularity was expanded in Ang1^{OE} mice (G-L). Unless otherwise denoted, *n*=4 per group. **P*<0.05 versus control. (A,B) Photographs showing gross features and inguinal WAT at E18.5. Scale bars: 1 mm. (C) Images of clusters in WAT stained for perilipin and CD31. Scale bars: 100 µm. (D) Comparison of the number of perilipin^{+} cells per cluster at E18.5. (E,F) Quantitative real-time PCR analyses of *Vegfr2* and *Pparg2* in WAT at E18.5. *n*=5 per group. (G,H) Photographs showing gross features and inguinal WAT of control and Ang1^{OE} embryos at E18.5. Arrows indicate a reddish skin color due to increased vascularity and vessel enlargement. Scale bars: 1 mm. (I) Images of clusters in WAT of control and Ang1^{OE} at E18.5 stained for perilipin and CD31. Scale bars: 100 µm. (J) Comparison of the number of perilipin^{+} cells per cluster at E18.5. (K,L) Quantitative real-time PCR analyses of *Vegfr2* and *Pparg2* in WAT at E18.5. Error bars represent s.d.

Development (2015) 142, 2623-2632 doi:10.1242/dev.125336

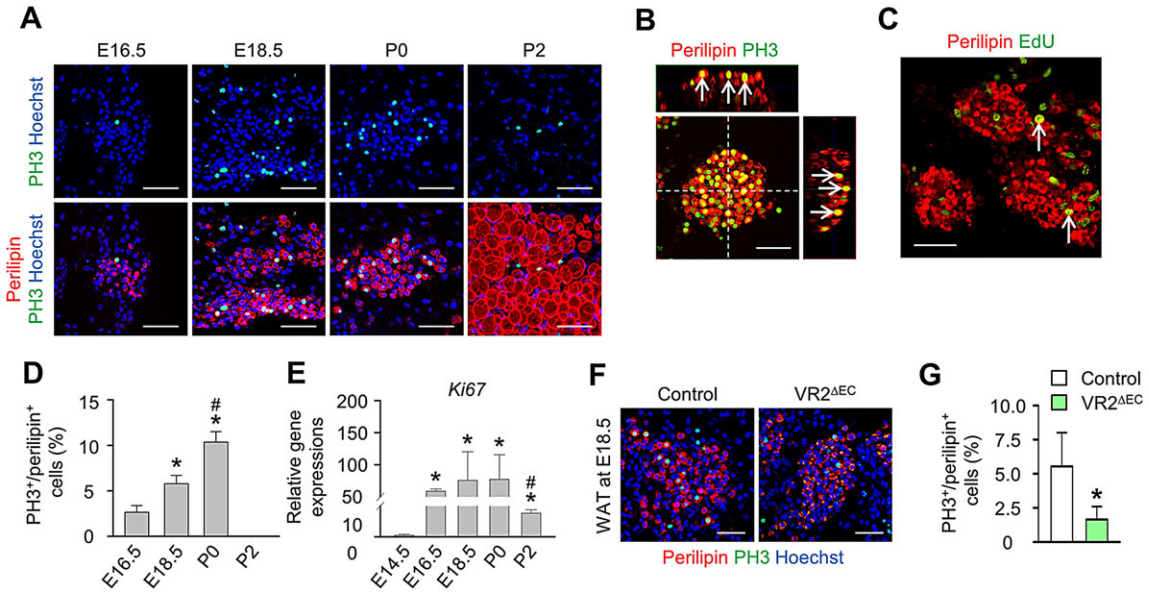

Fig. 3. Temporal changes of proliferative ability in PPAs. (A) Images showing perilipin$^+$ PH3$^+$ cells residing in adipose clusters at the indicated time points. (B) Image of orthotopically dissected cluster stained for perilipin and PH3. Arrows indicate perilipin$^+$ PH3$^+$ proliferating cells at the periphery of adipose cluster. (C) Image showing incorporated EdU signals (arrows) in adipose clusters at E18.5. (D) Comparison of the proportion of PH3$^+$ cells in perilipin$^+$ cells. *n*=8-10 per group. **P*<0.05 versus E16.5; $^{\#}$*P*<0.05 versus E18.5. (E) Quantitative real-time PCR analyses of *Ki67*. Samples were obtained from WAT at the indicated time points. *n*=4 per group. **P*<0.05 versus E14.5; $^{\#}$*P*<0.05 versus E16.5, E18.5 or P0. (F) Images showing perilipin$^+$ PH3$^+$ proliferating cells at E18.5 WAT of VR2$^{\Delta EC}$ embryos. (G) Comparison of the proportion of PH3$^+$ cells in perilipin$^+$ cells of VR2$^{\Delta EC}$ embryos. *n*=4 per group. **P*<0.05 versus VR2$^{\Delta EC}$. Error bars represent s.d. Scale bars: 50 µm.

consistent with the gene expression of another proliferation marker, *Ki67* (*Mki67* – Mouse Genome Informatics), in the inguinal WAT (Fig. 3E). However, the proportion of the proliferating cells decreased sharply when its cell size expanded, due to apparent lipid-fillings (Fig. 3A,D). To confirm this phenomenon *in vitro*, 3T3-L1 cells were cultured with adipogenic differentiation medium and observed at an early differentiation period. Consistently, perilipin$^+$ PPARγ$^+$ PH3$^+$ cells were detected at day 3 after adipogenic differentiation (supplementary material Fig. S2D), which was similar to the *in vivo* findings. To confirm this finding, we used a live-imaging device and were able to observe dividing cells containing scant lipid droplets that were stained with BODIPY in 3T3-L1 cells (supplementary material Fig. S2E). Furthermore, E18.5 WAT of VR2$^{\Delta EC}$ embryos showed a reduction in the number of PH3$^+$ cells in the PPA population by 70% compared with control embryos (Fig. 3F,G), indicating that actively growing vasculature is required for proper development of WAT through promotion of PPA proliferation.

Embryonic preadipocytes are different from adult preadipocytes

Lipid-lacking PPAs and adult preadipocytes can be enriched as adipose stromal vascular fraction (SVF), a heterogeneous mixture of cells operationally defined by enzymatic dissociation of WAT followed by density separation from lipid-retaining adipocytes (Han et al., 2011). To evaluate the differences between PPAs and adult preadipocytes, we first performed a colony-forming unit fibroblast (CFU-F) assay in WAT from E18.5 and adult inguinal WAT. Both SVFs could produce fibroblast colonies, but the number of colonies from E18.5 WAT was higher than that from adult WAT, whereas the sizes of adult colonies were relatively larger than those of E18.5 (Fig. 4A-C). Moreover, flow cytometry analyses with surface markers of mesenchymal and adipose stem cells [CD24, CD29 (Itgb1), CD34, Sca-1 (Ly6a) and PDGFRα] on a lineage-negative population [CD31$^-$ CD45$^-$ (Ptprc) Ter119$^-$ (Ly76)] revealed that CD24-, CD29-, CD34- and PDGFRα-expressing cells were highly enriched in the SVF of E18.5 WAT compared with the SVF of adult WAT (Fig. 4D,E). Our findings regarding the differences in preadipocyte characteristics between embryos and adults are in line with a recent report addressing two distinct adipose progenitor populations: developmental and adult (Jiang et al., 2014). As it was reported that the majority of adipose progenitors are derived from the PDGFRβ$^+$ mural cell compartment (Tang et al., 2008), we were curious about whether PPAs could share their origin and identity with the PDGFRβ$^+$ mural cell. To trace PDGFRβ$^+$ adipose progenitors, we intercrossed *Pdgfrb-Cre*-ER^{T2} and reporter *tdTomato* (supplementary material Fig. S3A,B) or *mT/mG* mice, and then administrated tamoxifen into a pregnant female at different time points (E10.5, E13.5 and E16.5) and analyzed inguinal WAT at E18.5 (Fig. 4F). We found that a subset of embryonic PDGFRβ$^+$ mural cells already had adipogenic potential. In contrast to the gradual increase in the number of GFP$^+$ pericytes or stromal cells during embryogenesis, the WAT of the embryos that were injected with tamoxifen at E13.5 had the highest number of GFP$^+$ cells in the perilipin$^+$ cell population at E18.5 (Fig. 4G-I), indicating that the conversion from PDGFRβ$^+$ cells to adipose-lineage cells either takes a few days or only occurs during specific periods. Despite this, and contrary to a previous study (Tang et al., 2008), the majority of embryonic preadipocytes inside the clusters were not derived from the PDGFRβ$^+$ mural cell compartment (Fig. 4G-I). These findings suggest that embryonic preadipocytes in WAT are derived from several subsets of mesenchymal cells.

Stepwise but dynamic regulation of preadipocyte formation and differentiation during embryogenesis

To gain insight into the detailed characteristics of PPAs, we harvested and cultured the SVF of inguinal WAT obtained at each prenatal period. Under adipogenic differentiation medium, SVFs

Development (2015) 142, 2623-2632 doi:10.1242/dev.125336

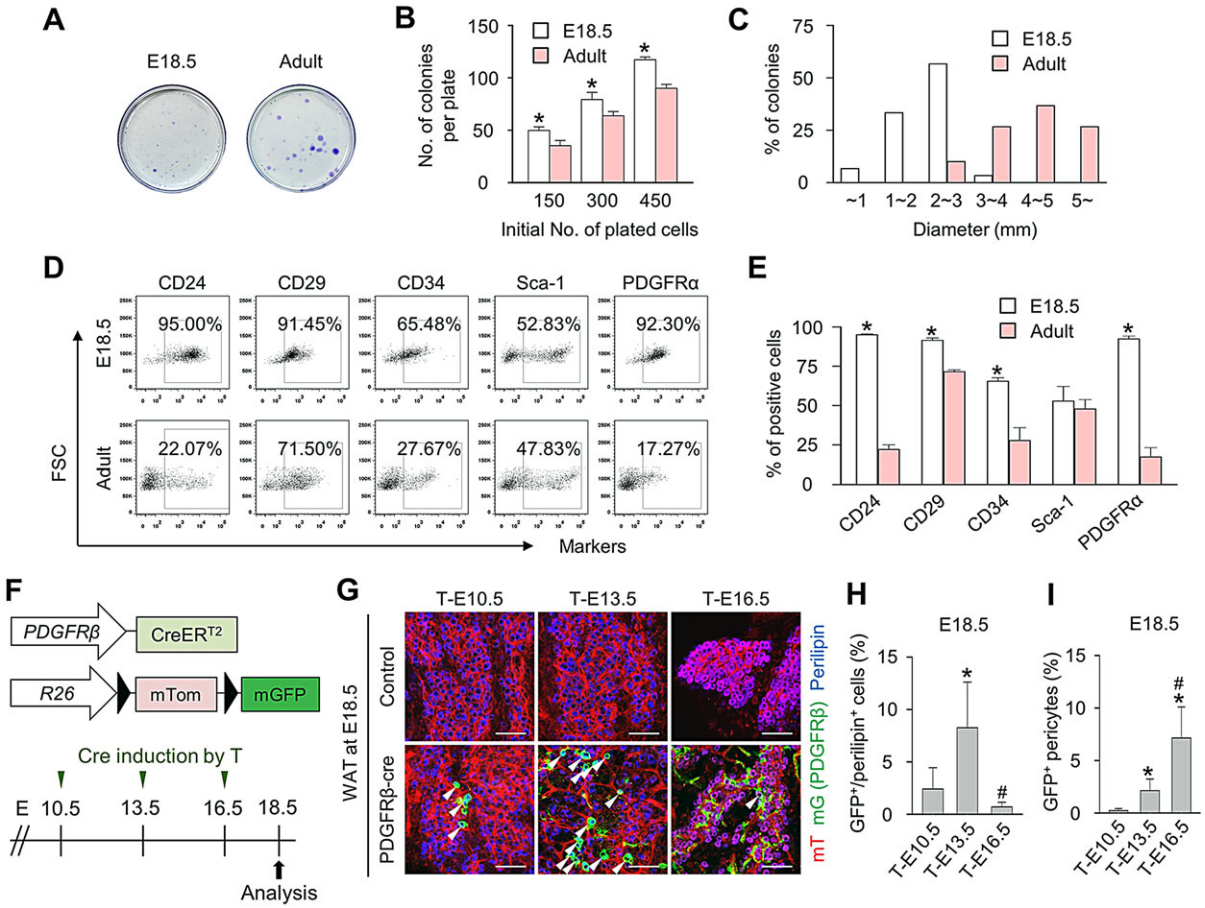

Fig. 4. Comparison of preadipocyte characteristics of embryos and adults. (A-C) Fibroblast colony formation with SVF cells derived from WAT of E18.5 and adult mice (2 months old). Crystal Violet staining was used to visualize colonies. *n*=4 per group. **P*<0.05 versus adult. Error bars represent s.d. (A) Photograph of SVF cells with Crystal Violet staining. (B,C) Comparisons of the numbers and diameters of colonies obtained from E18.5 and adult mice. **P*<0.05 versus adult. (D) Representative dot plots of SVF cells with surface markers CD24, CD29, CD34, Sca-1 and PDGFRα in flow cytometry analyses among lineage-negative population (CD31$^-$ CD45$^-$ Ter119$^-$) at E18.5 and adulthood. (E) Comparisons of the expression levels of CD24, CD29, CD34, Sca-1 and PDGFRα among lineage-negative population at E18.5 and adulthood. **P*<0.05 versus adult. (F,G) Lineage-tracing studies of PDGFRβ-derived cells in inguinal WAT during embryogenesis. (F) Pregnant females having *PDGFRβ-Cre*-ER^{T2}/*mT*/*mG* embryos were divided into three groups, and received tamoxifen injection at E10.5, E13.5 or E16.5 (designated T-E10.5, T-E13.5 and T-E16.5, respectively) and were analyzed at E18.5. (G) Images of perilipin$^+$ GFP$^+$ cells (arrowheads) in clusters of WAT at E18.5. Scale bars: 50 µm. (H,I) Comparisons of the proportion of GFP$^+$ cells in perilipin$^+$ cells and GFP$^+$ pericytes at E18.5. *n*=5 per group. **P*<0.05 versus tamoxifen injection at E10.5; $^{\#}$*P*<0.05 versus tamoxifen injection at E13.5.

were evidently differentiated into Oil Red O$^+$ lipid-filling cells at day 7. This adipose-lineage commitment started from E14.5, and robustly occurred after E16.5 (Fig. 5A,B). Quantitative real-time PCR analyses on the expression of key adipogenic molecules and markers in the SVF indicated that the gene expression levels of preadipocyte/adipocyte markers, such as *Cebpb*, *Pparg2* and *Cebpa*, increased markedly, showing the highest peak at E18.5, and the expression of *Plin1* elevated significantly after P0 (Fig. 5C). Consistent with the gene expression patterns, immunostaining for adipogenic transcription factors inside the cluster showed prominent PPARγ and C/EBPα protein expression after E16.5 (Fig. 5D,E). Interestingly, most PPARγ$^+$ or C/EBPα$^+$ cells already co-expressed perilipin (Fig. 5D,E), implying that this adipogenic transcriptional cascade actively occurs in the PPAs several days before birth. Moreover, the deposition of laminin-containing basement membrane was not distinctly found in PPAs at E16.5, whereas it was distinct on the margin of PPAs at P0 (Fig. 5F). By comparison, integrin α5, a receptor for fibronectin that is known to be expressed in preadipocytes but not in adipocytes (Liu et al., 2005), was highly present in PPAs at E16.5, whereas it was low in PPAs at P0 (Fig. 5G). To characterize PPAs further, we performed *ex vivo* culture of clusters derived from embryonic WAT. Plating the clusters induced cell proliferation around the cluster within a few days (supplementary material Fig. S4A). By Oil Red O staining, we noticed distinct cell populations inside and outside of the cluster. Because the cells inside the cluster were stained with Oil Red O without adipogenic differentiation medium, Oil Red O$^+$ cells were regarded as nascent adipocytes that accumulated lipid during the culture (supplementary material Fig. S4A). However, as Oil Red O$^+$ cells outside the cluster were present only under adipogenic differentiation medium (supplementary material Fig. S4A), these migrated Oil Red O$^+$ cells outside the cluster were regarded as preadipocytes that were differentiated into adipocytes when cultured with adipogenic differentiation supplementation. Surprisingly, some of the migrated cells outside the cluster without adipogenic differentiation medium were stained with perilipin and PH3 (supplementary material Fig. S4B). Taken together, these findings revealed that the embryonic preadipocytes with proliferative and migrative capacity express perilipin, which is again contrary to the notion that perilipin is exclusively expressed by differentiated

Development (2015) 142, 2623-2632 doi:10.1242/dev.125336

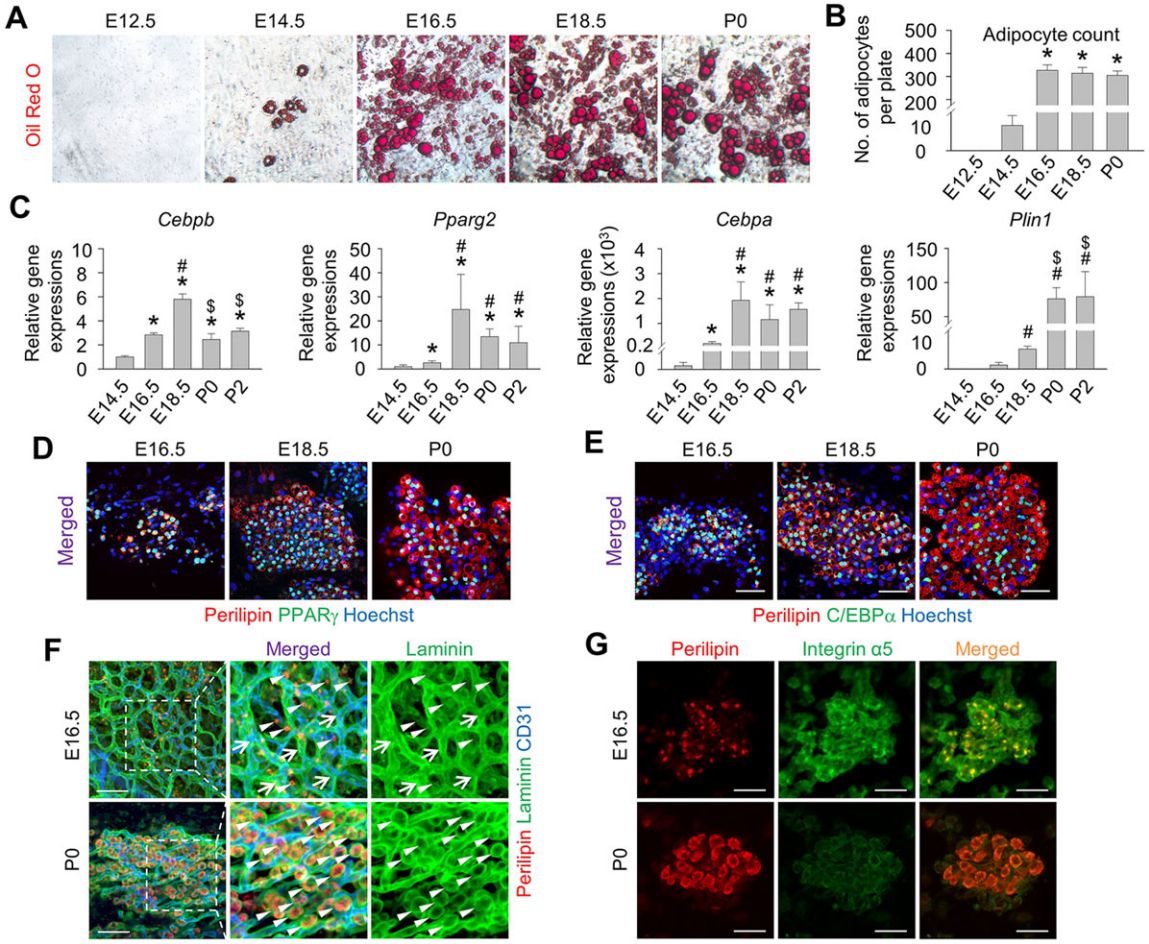

Fig. 5. Stepwise regulation of preadipocyte formation and differentiation during embryogenesis. (A,B) SVF cells derived from inguinal WAT at the indicated time points were harvested and cultured until confluent. On post-confluent day 2, the culture medium was replaced with adipogenic differentiation medium and the differentiated adipocytes were quantified at day 7. (A) Photographs of lipid-filled adipocytes shown by Oil Red O staining. (B) Comparison of the numbers of lipid-filled adipocytes per plate in the SVF cells obtained from the indicated time points. *n*=5 per group. **P*<0.05 versus E14.5. (C) Quantitative real-time PCR analyses of *Cebpb*, *Pparg2*, *Cebpa* and *Plin1* in inguinal WAT at the indicated time points. *n*=4 per group. **P*<0.05 versus E14.5; $^{\#}$*P*<0.05 versus E16.5; $^{\$}$*P*<0.05 versus E18.5. (D,E) Images of clusters containing perilipin^{+} PPARγ^{+} cells and perilipin^{+} C/EBPα^{+} cells at the indicated time points. Scale bars: 50 µm. (F) Images of inguinal WATs at E16.5 and P0 stained for perilipin, laminin and CD31. (Top) Arrowheads indicate perilipin^{+} laminin^{-} cells, whereas arrows indicate laminin^{+} adipose vasculatures. (Bottom) Arrowheads indicate perilipin^{+} laminin^{+} cells. Scale bars: 50 µm. (G) Images of clusters stained with perilipin and integrin α5. Scale bars: 25 µm.

adipocytes. Taken together, these findings indicate that there is a stepwise regulation of preadipocyte formation and differentiation during embryogenesis.

The adiponectin^{+} preadipocytes are almost identical to PPAs

To validate our findings, we evaluated the expression of adiponectin, which is a selective marker for adipocyte differentiation as well as a well-known adipokine, in PPAs of *adiponectin-Cre/tdTomato* (Ad-Tomato) mice. In Ad-Tomato embryos, tdTomato signal was highly detected in the inguinal WAT at E18.5, and PH3^{+} proliferating PPAs were frequently detected in the adiponectin^{+} PPA population at the inside of clusters (Fig. 6A). By immunostaining the cultured PPAs of Ad-Tomato embryos, we found a mixed population of fibroblast-like shaped adiponectin^{+} integrin α5^{high} preadipocytes and round shaped adiponectin^{+} integrin α5^{low} adipocytes, which were distinguishable by morphology (Fig. 6B). A subset of cultured adiponectin^{+} cells were perilipin^{+} and small lipid droplet-containing preadipocytes, and were also PPARγ^{+} and PH3^{+} proliferating preadipocytes (supplementary material Fig. S5A,B). Furthermore, like perilipin^{+} SVF cells (supplementary material Fig. S6, S7), more than 50% of adiponectin^{+} SVF cells also co-expressed CD24, CD29, CD34, Sca-1 and PDGFRα (Fig. 6C,D).

Next, we investigated the differences in the functional capacity between adiponectin^{+} preadipocytes and adiponectin^{-} SVF cells. After digesting E18.5 WAT of Ad-Tomato embryos, we harvested and plated the SVF cells for 1 day to eliminate any existing hematopoietic cells (Gupta et al., 2012). Flow cytometry analysis showed two distinct populations of adiponectin^{+} cell and adiponectin^{-} cells by the intensity of tdTomato signal; 10.3% of cultured SVF cells were adiponectin^{+} cells (Fig. 6E). We then sorted these two populations and plated and cultured them with adipogenic differentiation medium. The gene expression levels of tdTomato and adiponectin confirmed that sorted tdTomato^{+} SVF cells showed enrichment for adiponectin (Fig. 6H). As we expected, most of the sorted tdTomato^{+} SVF cells expressed strong tdTomato signal with a fibroblast-like cell shape in the undifferentiated state, suggesting that they are adiponectin^{+} preadipocytes (Fig. 6F). During adipogenic differentiation, tdTomato^{+} preadipocytes were robustly differentiated into Oil Red O^{+} adipocytes, to a greater extent than adiponectin^{-} cells (Fig. 6G; supplementary material Fig. S5C,D).

Development (2015) 142, 2623-2632 doi:10.1242/dev.125336

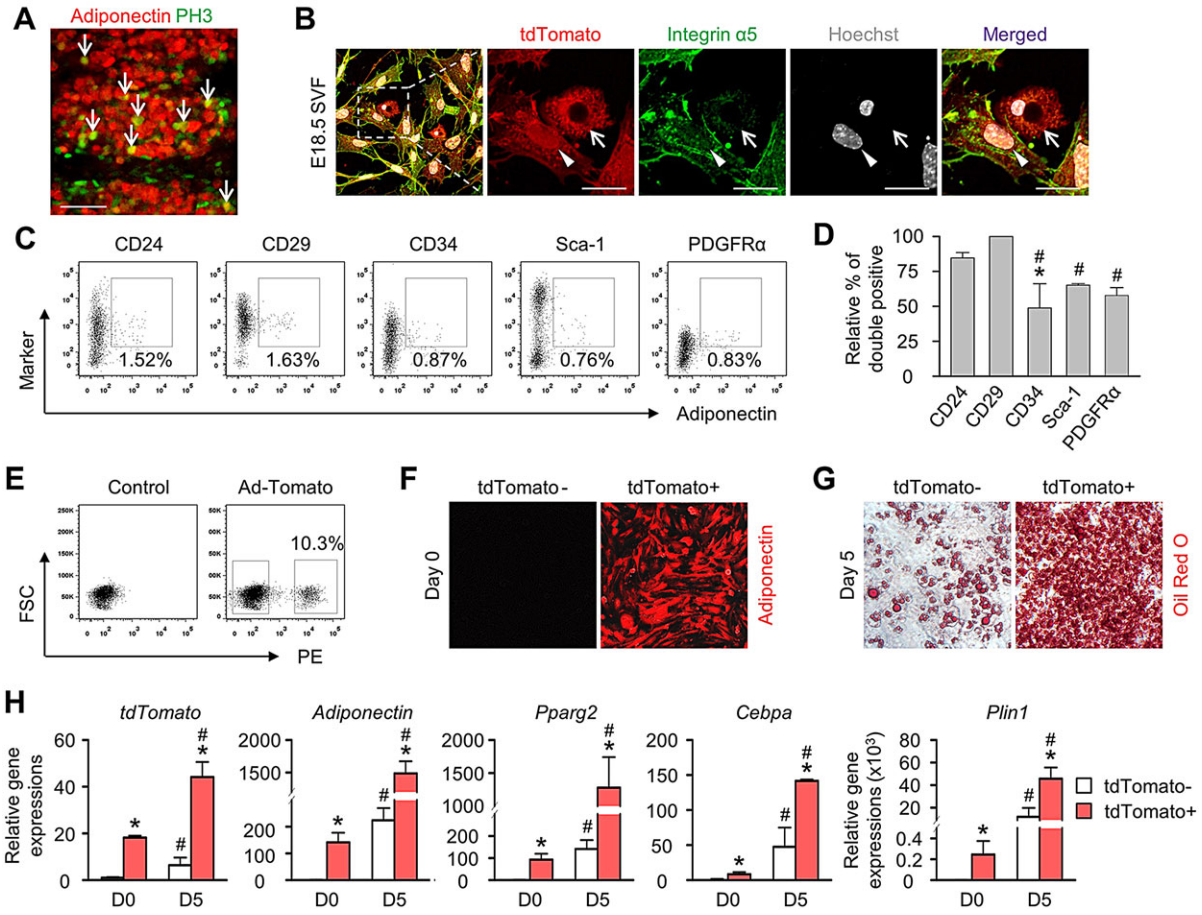

Fig. 6. Preadipocytes are enriched within adiponectin^{+} subset of embryonic SVF cells. Embryos and SVF cells were harvested from *adiponectin-Cre*/*tdTomato* (Ad-Tomato) mice. (A) Image of adipose clusters at E18.5. Arrows indicate PH3^{+} proliferating adiponectin^{+} preadipocytes. Scale bar: 50 µm. (B-H) The SVF cells derived from E18.5 inguinal WAT were harvested and sorted into tdTomato^{-} and tdTomato^{+} cells. Each group was plated and cultured with adipogenic differentiation medium for 3 days, and replaced with maintenance medium. *n*=4 per group. (B) Images of tdTomato^{+} cells stained with integrin α5. Arrow indicates tdTomato^{+} integrin α5^{-} adipocyte, and arrowhead indicates tdTomato^{+} integrin α5^{+} preadipocyte. Scale bars: 20 µm. (C) Flow cytometry plots of tdTomato^{+} SVF cells with the surface markers CD24, CD29, CD34, Sca-1 and PDGFRα among a lineage-negative population. (D) Relative proportion of cells with CD24, CD29, CD34, Sca-1 and PDGFRα in tdTomato^{+} SVF cells. **P*<0.05 versus CD24; $^{\#}$*P*<0.05 versus CD29. (E) Flow cytometry plots of cultured SVF cells from E18.5 inguinal WAT of control and Ad-Tomato embryos. tdTomato^{-} and tdTomato^{+} population were collected based on the tdTomato intensity of control SVF cells. (F) Images of sorted tdTomato^{-} and tdTomato^{+} cells before adipogenic differentiation. (G) Photographs of Oil Red O staining of tdTomato^{-} and tdTomato^{+} SVF cells 5 days after adipogenic differentiation. (H) Quantitative real-time PCR analyses of *tdTomato*, *adiponectin*, *Pparg2*, *Cebpa* and *Plin1* in tdTomato^{-} and tdTomato^{+} SVF cells with (D5) or without (D0) adipogenic differentiation. **P*<0.05 versus tdTomato^{-} SVF cells; $^{\#}$*P*<0.05 versus undifferentiated SVF cells.

The quantitative differences of adipocytes between the two populations were matched with the gene expression levels of *Plin1* (Fig. 6H). Moreover, the gene expression levels of preadipocyte/adipocyte markers, such as *Pparg2* and *Cebpa*, displayed markedly increased patterns from tdTomato^{+} embryonic SVF cells in both the undifferentiated and differentiated states (Fig. 6H). Thus, the adiponectin^{+} cells are almost identical to PPAs. Collectively, these data indicate the similarity between perilipin^{+} cells and adiponectin^{+} cells as embryonic preadipocytes.

DISCUSSION

In this study, we demonstrate that embryonic perilipin^{+} preadipocytes in WAT proliferate to form clusters and interact with growing adipose vasculature (which is at odds with the previously held belief that perilipin is expressed exclusively in differentiated adipocytes) and that they proliferate robustly within a few days during the prenatal period. In turn, generation of a massive quantity of PPAs during the prenatal period could be a prerequisite to building a certain size of WAT rapidly with fully lipid-filled, differentiated adipocytes by consumption of lipid-rich nutrients such as milk during the postnatal period.

Accumulating evidence demonstrates that adipose tissue expansion and remodeling is angiogenesis dependent during the postnatal period and adulthood (Rupnick et al., 2002; Cao, 2007; Cho et al., 2007; Sun et al., 2011). The closed structural relationship between adipocytes and vasculature facilitates constant and immediate responses to various conditions to maintain metabolic homeostasis. In addition to its basic roles, the adipose vasculature has important roles in providing hormones, growth factors, inflammation-related cytokines, and stem cells to adipose tissues (Nishimura et al., 2009; Christiaens and Lijnen, 2010; Cao, 2013). Our findings indicate that the role of the growing vasculature as an adipose niche applies also to the growth of PPAs as a cluster during embryogenesis.

Preadipocytes enter the cell cycle, go through one or two rounds of replication that is called mitotic clonal expansion, and proceed to terminal differentiation *in vitro* (Tang et al., 2003). However, little is known about whether this event is a prerequisite for adipogenic

Development (2015) 142, 2623-2632 doi:10.1242/dev.125336

differentiation, and whether it takes place *in vivo*. Our findings demonstrate the existence of preadipocytes that undergo active proliferation in embryonic WAT, which might be considered as an *in vivo* mitotic clonal expansion. Furthermore, the observation of proliferative perilipin^{+} or adiponectin^{+} cells conflict with the current consensus that perilipin or adiponectin is expressed exclusively in differentiated adipocytes, which have lost their proliferation abilities (Greenberg et al., 1991; Cawthorn et al., 2012). Yet, it is reported that rapid cellular turnover occurs in adipose tissues, in which subsets of C/EBPα^{+} or PPA cells expressed proliferative markers, such as Ki67 or BrdU, as well as in ob/ob mice (Rigamonti et al., 2011). Furthermore, EdU^{+} proliferating cells expressed perilipin during the initial phase of browning initiated by stimulation with a β3 agonist (Lee et al., 2012). These previous observations, as well as our findings, can be interpreted as the existence of preadipocytes expressing differentiated adipocyte markers or adipocytes expressing proliferative markers in embryonic WAT.

To characterize the observed PPAs in more detail, we collected evidence to support our hypothesis. First, both cultured PPAs and adiponectin^{+} preadipocytes evidently showed a typical fibroblast-like shape and robust adipogenic differentiation under adipogenic medium differentiation. Second, partially differentiated human preadipocytes have been shown to still be capable of cell division (Prins and O'Rahilly, 1997; Gregoire et al., 1998). These reports are in line with our findings that a subset of PPAs, without noticeable lipid droplets, also divided under adipogenic differentiation. Third, the differences in laminin deposition and integrin α5 expression in PPAs between E16.5 and P0 indicate the onset of prenatal adipogenesis, which is usually defined by extracellular matrix remodeling and characterized by the conversion from the fibronectin-rich stromal matrix to a laminin-rich basement membrane (Liu et al., 2005; Hoshiba et al., 2010). Together, we can conclude that a subset of preadipocytes expressing differentiated adipocyte markers resides in the embryonic WAT.

A recent report demonstrated that there is a decrease in the expression of CD24, one of the stem cell markers, in preadipocytes after birth (Berry and Rodeheffer, 2013). Likewise, we also observed differences in the expression of stem cell markers (CD24, CD29, CD34 and PDGFRα) between E18.5 and adult. Moreover, we discovered that a small number of embryonic preadipocytes was derived from the PDGFRβ^{+} mural cell compartment by using *Pdgfrb-Cre*-ER^{T2} reporter mice, in contrast to a previous report that observed *lacZ* expression in P30 WAT under the control of *Pdgfrb-Cre* (Tang et al., 2008). Considering recent studies stating that region, sex, strain, age and nutrition can affect the gene expression and physiological phenotypes of adipose tissue as well as the quantity of adipose progenitors (Yamamoto et al., 2010; Macotela et al., 2012; Chau et al., 2014), we also propose that the preadipocyte populations in WAT of embryos and adults are different in character, and even origin.

Like stem cell markers such as CD24, CD29 and CD34, perilipin has been used as marker of prenatal preadipocytes for this study. As perilipin knockout mice showed reduced body weight and resistance to diet-induced obesity (Tansey et al., 2001), which indicates alterations in metabolic homeostasis, elaborative studies on time- and tissue-specific ablation of perilipin by genetically modified mice will be required to understand the roles of perilipin in preadipocytes.

In conclusion, we demonstrate that the expression of perilipin or adiponectin is not confined to terminally differentiated adipocytes. Rather, embryonic preadipocytes expressing these markers proliferate in order to expand the adipose-lineage cell population. Although subsequent studies are required to explore the underlying mechanisms, we highlight the role of embryonic preadipocytes and the prenatal period in the control of *in vivo* adipogenesis, which we believe will subsequently open new directions to exploring the cause of obesity.

MATERIALS AND METHODS

Animals

Specific pathogen-free C57BL/6J, *Adiponectin-Cre* and *tdTomato* mice were purchased from Jackson Laboratory; *Pdgfrb-Cre*-ER^{T2} transgenic mice used in this study contained a BAC construct of *Pdgfrb* and the tamoxifen-inducible Cre recombinase (Feil et al., 1997; Stanczuk et al., 2015; R. H. Adams, unpublished). *VEGFR2*$^{+/fl}$ (Albuquerque et al., 2009) mice were kindly provided by Professor Masanori Hirashima (Kobe University, Japan). *VE-Cadherin-Cre*-ER^{T2} (Wang et al., 2010), *Col1a1-Cre* (Liu et al., 2004), inducible *COMP-Ang1*-Tg (Lee et al., 2013) and *mT/mG* (Muzumdar et al., 2007) mice were transferred and bred in our specific pathogen-free animal facilities at KAIST. Tamoxifen (Sigma-Aldrich) was dissolved in corn oil and administrated into the peritoneal cavity of pregnant females (3.0 mg/mouse) at the indicated time point. Embryos in this study were generated by timed mating, and E0.5 was regarded as the day of prominent plug formation. Mice from E12.5 to 2-month-old adults were used for this study. All mice were bred in our specific pathogen-free animal facility and were fed normal chow diet (NCD) (PMI LabDiet) with *ad libitum* access to water. Animal care and experimental procedures were performed under the approval from the Institutional Animal Care and Use Committee (No. KA2013-37) of KAIST.

Histological analysis

Mice were anesthetized with a combination of ketamine (80 mg/kg) and xylazine (12 mg/kg) by intramuscular injection. All adipose tissues were from male adult mice, or from embryos or pups regardless of gender. Harvested tissues were fixed with 4% paraformaldehyde in PBS for 1 h, and whole-mounted or cryo-embedded followed by cryosectioning. After blocking with 5% goat or donkey serum (Jackson ImmunoResearch) in PBST (0.3% Triton X-100 in PBS for whole-mount method, 0.03% Triton X-100 in PBS for cryosections) for 1 h at room temperature, whole-mounted or sectioned tissue was incubated overnight with primary antibodies (supplementary material Table S1) at 4°C. After several washes with PBST, the samples were incubated with the following secondary antibodies (supplementary material Table S2) for 2 h at room temperature: Cy3-, Cy5- or FITC-conjugated goat anti-guinea pig antibody; Cy3- or Cy5-conjugated goat anti-hamster antibody; Cy3-, Cy5- or FITC-conjugated goat anti-rabbit antibody; Cy3- or FITC-conjugated goat anti-rat antibody; and Cy3- or FITC-conjugated donkey anti-goat antibody. Hoechst 33342 (Sigma-Aldrich) was used to detect nuclei, and boron-dipyrromethene (BODIPY, Invitrogen) was used to detect lipid droplets in adipocytes. For flash-labeling, prepared mice were injected intraperitoneally with 5-ethynyl-2′-deoxyuridine (EdU; 2 nmol/mouse; Invitrogen) and sacrificed after the indicated interval. EdU was detected according to the manufacturer's instructions. For cell staining, cells at the indicated time points were fixed with 4% paraformaldehyde in PBS for 1 h, blocked with 5% goat serum in PBST, and stained with antibodies (supplementary material Table S1). To label proliferating cells, 3T3-L1 cells were incubated with 10 μM EdU (Invitrogen) for 3 h and processed for EdU detection and staining.

Morphometric analysis

Confocal microscopes (ApoTome, LSM 510 and LSM 780, Carl Zeiss) equipped with argon and helium-neon lasers were used to visualize fluorescence images. Morphometric analyses were performed with Image J software (NIH) or Zeiss image software (ZEN 2012).

In vitro culture of 3T3-L1 cell line

The 3T3-L1 cell line was maintained in culture medium, which is a mixture of 10% calf serum and 100 μg/ml streptomycin in Dulbecco's modified Eagle medium (DMEM). In order to induce adipogenic differentiation, 2-day-postconfluent cells were incubated with adipogenic differentiation medium

Development (2015) 142, 2623-2632 doi:10.1242/dev.125336

[DMEM containing 10% fetal bovine serum, 5 µg/ml insulin (Sigma-Aldrich), 0.5 mM 3-isobutyl-1-methylxanthine (IBMX, Sigma-Aldrich) and 1 µM dexamethasone (Sigma-Aldrich)]. After 3 days, adipogenic differentiation medium was replaced with maintenance medium (DMEM containing 10% fetal bovine serum and 5 µg/ml insulin).

In vitro culture of SVF and *ex vivo* culture of clusters

Dissected inguinal WAT samples were chopped with scissors and incubated in digestion medium containing DMEM/F12 with 5 µg/ml insulin (Sigma-Aldrich), 100 U/ml hyaluronidase (Sigma-Aldrich), 10 ng/ml EGF (Sigma-Aldrich), 20 ng/ml cholera toxin (Sigma-Aldrich), 5% FBS, 500 ng/ml hydrocortisone (Sigma-Aldrich), 100 µg/ml streptomycin and 300 U/ml collagenase-1A (Sigma-Aldrich) for 1 h at 37°C. The resulting suspension was dissociated with 0.5 ml 0.25% trypsin/EDTA (Life Technologies) for 1.5 min at 37°C, and sequentially re-suspended in 0.1 mg/ml DNase for 5 min at 37°C. Erythrocytes were lysed with ACK Lysing Buffer (Life Technologies) for 5 min at 37°C and centrifuged at 470 ***g*** for 5 min. After several washes, the SVF pellet was re-suspended in culture medium. Two days after confluency was observed, SVF cells were cultured with adipogenic differentiation medium. After 3 days, adipogenic differentiation medium was changed to maintenance medium. For *ex vivo* culture of clusters, dissected adipose tissues derived from E18.5 embryos were incubated with HBSS containing 0.2% collagenase type II for 10 min at room temperature. Using sharp scissors under the microscope, clusters then were excised, trimmed, and plated in culture containing DMEM supplemented with 10% bovine serum.

Colony-forming unit fibroblast (CFU-F) assay

To quantify the proliferative activity of mesenchymal stem cells, we sorted lineage-negative SVF cells ($CD31^-$ $CD45^-$ $Ter119^-$) from E18.5 and adult (2 months old) subcutaneous adipose tissue using FACSAria II (BD Biosciences) with the listed antibodies (supplementary material Table S1). Sorted cells (150, 300 or 450 per 100-mm plate) were seeded with culture medium. Without adipogenic differentiation, cells were grown for 14 days and fixed with 4% paraformaldehyde for 10 min. The number and size of colonies were assessed after staining with Crystal Violet (Sigma-Aldrich).

Live cell imaging

3T3-L1 or SVF cells were cultured in 6-well plates with or without adipogenic differentiation. Using an incubator chamber (Live Cell Instrument) equipped with optimal environment settings of 5% CO_2 and 37°C, live cell imaging was performed and recorded at 5 or 10 min intervals by microscope (ApoTome, Carl Zeiss) equipped with argon and helium-neon lasers.

Flow cytometry analysis

SVF cells of E16.5, E18.5, P0, P2 and adult (2 months old) were harvested by digestion of subcutaneous adipose tissue. SVF was sequentially filtered through 70- and 40-µm filters. For intracellular staining, Cytofix/Cytoperm kit (BD Biosciences) was used according to the manufacturer's instructions. Before incubation with antibodies, Fc receptors were blocked with CD16/CD32 antibody for 10 min to minimize non-specific binding. Cells were incubated with antibodies at 4°C for 30 min. Following antibody incubation, samples were washed, centrifuged at 300 ***g*** for 3 min and resuspended in PBS containing 5% calf serum (see supplementary material Table S1 for antibodies). The lineage-negative population was analyzed with FACSAria II (BD Biosciences). Data analysis was performed with FlowJo software (Tree Star).

Oil Red O staining

The cells in the wells were fixed with 4% paraformaldehyde for 40 min at room temperature. After being washed with PBS and 60% isopropanol, cells were incubated with filtered Oil Red O working solution for 50 min at room temperature. After staining, several washes with PBS and 60% isopropanol were performed to reduce non-specific staining. Images of stained cells were captured by a microscope equipped with a CCD camera (Carl Zeiss).

X-gal staining

Adipose tissues derived from *VEGFR2*$^+$*/lacZ* mice were harvested, fixed with 4% paraformaldehyde in PBS for 1 h, and whole-mounted or cryo-embedded followed by cryosectioning. After several washes, whole or sliced tissues were incubated with X-gal working solution (Biosesang, Korea) at 37°C until galactosidase expression (indicated by blue color) was prominent. The staining was imaged using a microscope equipped with a CCD camera (Carl Zeiss).

RNA extraction and quantitative real-time PCR

Total RNA was extracted from adipose tissues with the RNeasy Plus Mini Kit (Qiagen) according to the manufacturer's instructions. Then, the mRNA was reverse-transcribed into cDNA using the GoScript Reverse Transcription Kit (Promega). Quantitative real-time PCR was performed with the indicated primers using the Bio-RadTM CFX96 Real-Time PCR Detection System (Bio-Rad; see supplementary material Table S3 for primers). The PCR data were analyzed using Bio-Rad CFX Manager Software (Bio-Rad).

Statistics

Values are presented as mean±s.d. Significant differences in the mean values were analyzed by the Mann–Whitney *U*-test or Kruskal–Wallis test followed by Tukey's post hoc test.

Acknowledgements

We are grateful to Hana Yoo, Sujin Seo and Sammi Yu for their technical assistance; and Masanori Hirashima (Kobe University, Japan) for *VEGFR2*$^{+/fl}$ mice.

Competing interests

The authors declare no competing or financial interests.

Author contributions

K.Y.H. designed, organized and performed the experiments, and generated the figures. K.Y.H., H.B. and I.P. wrote the manuscript. H.B., D.-Y.P., K.H.K., Y.K., H.K. and R.H.A. interpreted the data, and E.-S.C. generated Ang1 overexpression mouse. O.-J.Y. and G.Y.K. supervised the project and wrote the manuscript.

Funding

This research was supported by a grant from the Korean Healthcare Technology R&D Project, Ministry of Health and Welfare, Korea [A120275 to G.Y.K.]; and by the National Research Foundation (NRF) of Korea funded by the Ministry of Science, ICT & Future Planning, Korea [2013-036-003 to G.Y.K.].

Supplementary material

Supplementary material available online at
http://dev.biologists.org/lookup/suppl/doi:10.1242/dev.125336/-/DC1

References

Albuquerque, R. J. C., Hayashi, T., Cho, W. G., Kleinman, M. E., Dridi, S., Takeda, A., Baffi, J. Z., Yamada, K., Kaneko, H., Green, M. G. et al. (2009). Alternatively spliced vascular endothelial growth factor receptor-2 is an essential endogenous inhibitor of lymphatic vessel growth. *Nat. Med.* **15**, 1023-1030.

Berry, R. and Rodeheffer, M. S. (2013). Characterization of the adipocyte cellular lineage in vivo. *Nat. Cell Biol.* **15**, 302-308.

Birsoy, K., Berry, R., Wang, T., Ceyhan, O., Tavazoie, S., Friedman, J. M. and Rodeheffer, M. S. (2011). Analysis of gene networks in white adipose tissue development reveals a role for ETS2 in adipogenesis. *Development* **138**, 4709-4719.

Cao, Y. (2007). Angiogenesis modulates adipogenesis and obesity. *J. Clin. Invest.* **117**, 2362-2368.

Cao, Y. (2010). Adipose tissue angiogenesis as a therapeutic target for obesity and metabolic diseases. *Nat. Rev. Drug Discov.* **9**, 107-115.

Cao, Y. (2013). Angiogenesis and vascular functions in modulation of obesity, adipose metabolism, and insulin sensitivity. *Cell Metab.* **18**, 478-489.

Cawthorn, W. P., Scheller, E. L. and MacDougald, O. A. (2012). Adipose tissue stem cells meet preadipocyte commitment: going back to the future. *J. Lipid Res.* **53**, 227-246.

Chau, Y.-Y., Bandiera, R., Serrels, A., Martínez-Estrada, O. M., Qing, W., Lee, M., Slight, J., Thornburn, A., Berry, R., McHaffie, S. et al. (2014). Visceral and subcutaneous fat have different origins and evidence supports a mesothelial source. *Nat. Cell Biol.* **16**, 367-375.

Cho, C.-H., Koh, Y. J., Han, J., Sung, H.-K., Jong Lee, H., Morisada, T., Schwendener, R. A., Brekken, R. A., Kang, G., Oike, Y. et al. (2007).

Development (2015) 142, 2623-2632 doi:10.1242/dev.125336

Angiogenic role of LYVE-1-positive macrophages in adipose tissue. *Circ. Res.* **100**, e47-e57.

Christiaens, V. and Lijnen, H. R. (2010). Angiogenesis and development of adipose tissue. *Mol. Cell. Endocrinol.* **318**, 2-9.

Crandall, D. L., Hausman, G. J. and Kral, J. G. (1997). A review of the microcirculation of adipose tissue: anatomic, metabolic, and angiogenic perspectives. *Microcirculation* **4**, 211-232.

Feil, R., Wagner, J., Metzger, D. and Chambon, P. (1997). Regulation of Cre recombinase activity by mutated estrogen receptor ligand-binding domains. *Biochem. Biophys. Res. Commun.* **237**, 752-757.

Gesta, S., Tseng, Y.-H. and Kahn, C. R. (2007). Developmental origin of fat: tracking obesity to its source. *Cell* **131**, 242-256.

Greenberg, A. S., Egan, J. J., Wek, S. A., Garty, N. B., Blanchette-Mackie, E. J. and Londos, C. (1991). Perilipin, a major hormonally regulated adipocyte-specific phosphoprotein associated with the periphery of lipid storage droplets. *J. Biol. Chem.* **266**, 11341-11346.

Gregoire, F. M., Smas, C. M. and Sul, H. S. (1998). Understanding adipocyte differentiation. *Physiol. Rev.* **78**, 783-809.

Gupta, R. K., Mepani, R. J., Kleiner, S., Lo, J. C., Khandekar, M. J., Cohen, P., Frontini, A., Bhowmick, D. C., Ye, L., Cinti, S. et al. (2012). Zfp423 expression identifies committed preadipocytes and localizes to adipose endothelial and perivascular cells. *Cell Metab.* **15**, 230-239.

Han, J., Lee, J.-E., Jin, J., Lim, J. S., Oh, N., Kim, K., Chang, S.-I., Shibuya, M., Kim, H. and Koh, G. Y. (2011). The spatiotemporal development of adipose tissue. *Development* **138**, 5027-5037.

Hoshiba, T., Kawazoe, N., Tateishi, T. and Chen, G. (2010). Development of extracellular matrices mimicking stepwise adipogenesis of mesenchymal stem cells. *Adv. Mater.* **22**, 3042-3047.

Jiang, Y., Berry, D. C., Tang, W. and Graff, J. M. (2014). Independent stem cell lineages regulate adipose organogenesis and adipose homeostasis. *Cell Rep.* **9**, 1007-1022.

Lee, Y.-H., Petkova, A. P., Mottillo, E. P. and Granneman, J. G. (2012). In vivo identification of bipotential adipocyte progenitors recruited by beta3-adrenoceptor activation and high-fat feeding. *Cell Metab.* **15**, 480-491.

Lee, J., Kim, K. E., Choi, D.-K., Jang, J. Y., Jung, J.-J., Kiyonari, H., Shioi, G., Chang, W., Suda, T., Mochizuki, N. et al. (2013). Angiopoietin-1 guides directional angiogenesis through integrin alphavbeta5 signaling for recovery of ischemic retinopathy. *Sci. Transl. Med.* **5**, 203ra127.

Li, F. Y. L., Cheng, K. K., Lam, K. S. L., Vanhoutte, P. M. and Xu, A. (2011). Cross-talk between adipose tissue and vasculature: role of adiponectin. *Acta Physiol.* **203**, 167-180.

Liu, F., Woitge, H. W., Braut, A., Kronenberg, M. S., Lichtler, A. C., Mina, M. and Kream, B. E. (2004). Expression and activity of osteoblast-targeted Cre recombinase transgenes in murine skeletal tissues. *Int. J. Dev. Biol.* **48**, 645-653.

Liu, J., DeYoung, S. M., Zhang, M., Zhang, M., Cheng, A. and Saltiel, A. R. (2005). Changes in integrin expression during adipocyte differentiation. *Cell Metab.* **2**, 165-177.

Macotela, Y., Emanuelli, B., Mori, M. A., Gesta, S., Schulz, T. J., Tseng, Y.-H. and Kahn, C. R. (2012). Intrinsic differences in adipocyte precursor cells from different white fat depots. *Diabetes* **61**, 1691-1699.

Muzumdar, M. D., Tasic, B., Miyamichi, K., Li, L. and Luo, L. (2007). A global double-fluorescent Cre reporter mouse. *Genesis* **45**, 593-605.

Nedergaard, J. and Cannon, B. (2014). The browning of white adipose tissue: some burning issues. *Cell Metab.* **20**, 396-407.

Nishimura, S., Manabe, I., Nagasaki, M., Hosoya, Y., Yamashita, H., Fujita, H., Ohsugi, M., Tobe, K., Kadowaki, T., Nagai, R. et al. (2007). Adipogenesis in obesity requires close interplay between differentiating adipocytes, stromal cells, and blood vessels. *Diabetes* **56**, 1517-1526.

Nishimura, S., Manabe, I., Nagasaki, M., Eto, K., Yamashita, H., Ohsugi, M., Otsu, M., Hara, K., Ueki, K., Sugiura, S. et al. (2009). CD8+ effector T cells contribute to macrophage recruitment and adipose tissue inflammation in obesity. *Nat. Med.* **15**, 914-920.

Prins, J. B. and O'Rahilly, S. (1997). Regulation of adipose cell number in man. *Clin. Sci.* **92**, 3-11.

Rigamonti, A., Brennand, K., Lau, F. and Cowan, C. A. (2011). Rapid cellular turnover in adipose tissue. *PLoS ONE* **6**, e17637.

Rosen, E. D. and MacDougald, O. A. (2006). Adipocyte differentiation from the inside out. *Nat. Rev. Mol. Cell Biol.* **7**, 885-896.

Rosenwald, M., Perdikari, A., Rülicke, T. and Wolfrum, C. (2013). Bi-directional interconversion of brite and white adipocytes. *Nat. Cell Biol.* **15**, 659-667.

Rudolph, M. C., Neville, M. C. and Anderson, S. M. (2007). Lipid synthesis in lactation: diet and the fatty acid switch. *J. Mammary Gland Biol. Neoplasia* **12**, 269-281.

Rupnick, M. A., Panigrahy, D., Zhang, C.-Y., Dallabrida, S. M., Lowell, B. B., Langer, R. and Folkman, M. J. (2002). Adipose tissue mass can be regulated through the vasculature. *Proc. Natl. Acad. Sci. USA* **99**, 10730-10735.

Stanczuk, L., Martinez-Corral, I., Ulvmar, M. H., Zhang, Y., Lavina, B., Fruttiger, M., Adams, R. H., Saur, D., Betsholtz, C., Ortega, S. et al. (2015). cKit lineage hemogenic endothelium-derived cells contribute to mesenteric lymphatic vessels. *Cell Rep.* pii: S2211-1247(15)00172-2.

Sun, K., Kusminski, C. M. and Scherer, P. E. (2011). Adipose tissue remodeling and obesity. *J. Clin. Invest.* **121**, 2094-2101.

Tang, Q.-Q., Otto, T. C. and Lane, M. D. (2003). Mitotic clonal expansion: a synchronous process required for adipogenesis. *Proc. Natl. Acad. Sci. USA* **100**, 44-49.

Tang, W., Zeve, D., Suh, J. M., Bosnakovski, D., Kyba, M., Hammer, R. E., Tallquist, M. D. and Graff, J. M. (2008). White fat progenitor cells reside in the adipose vasculature. *Science* **322**, 583-586.

Tansey, J. T., Sztalryd, C., Gruia-Gray, J., Roush, D. L., Zee, J. V., Gavrilova, O., Reitman, M. L., Deng, C.-X., Li, C., Kimmel, A. R. et al. (2001). Perilipin ablation results in a lean mouse with aberrant adipocyte lipolysis, enhanced leptin production, and resistance to diet-induced obesity. *Proc. Natl. Acad. Sci. USA* **98**, 6494-6499.

Tran, K.-V., Gealekman, O., Frontini, A., Zingaretti, M. C., Morroni, M., Giordano, A., Smorlesi, A., Perugini, J., De Matteis, R., Sbarbati, A. et al. (2012). The vascular endothelium of the adipose tissue gives rise to both white and brown fat cells. *Cell Metab.* **15**, 222-229.

Wang, Y., Nakayama, M., Pitulescu, M. E., Schmidt, T. S., Bochenek, M. L., Sakakibara, A., Adams, S., Davy, A., Deutsch, U., Lüthi, U. et al. (2010). Ephrin-B2 controls VEGF-induced angiogenesis and lymphangiogenesis. *Nature* **465**, 483-486.

Wang, Q. A., Tao, C., Gupta, R. K. and Scherer, P. E. (2013). Tracking adipogenesis during white adipose tissue development, expansion and regeneration. *Nat. Med.* **19**, 1338-1344.

Wu, J., Boström, P., Sparks, L. M., Ye, L., Choi, J. H., Giang, A.-H., Khandekar, M., Virtanen, K. A., Nuutila, P., Schaart, G. et al. (2012). Beige adipocytes are a distinct type of thermogenic fat cell in mouse and human. *Cell* **150**, 366-376.

Yamamoto, Y., Gesta, S., Lee, K. Y., Tran, T. T., Saadatirad, P. and Ronald Kahn, C. (2010). Adipose depots possess unique developmental gene signatures. *Obesity* **18**, 872-878.